Journal of Energy Storage 12 (2017) 37–44

Contents lists available at ScienceDirect

Journal of Energy Storage

journal homepage: www.elsevier.com/locate/est

A detailed thermal study of usual $LiNi_{0.5}Co_{0.2}Mn_{0.3}O_2$, $LiMn_2O_4$ and $LiFePO_4$ cathode materials for lithium ion batteries

Yangyang Yu[a,1], Jing Wang[a,1], Peng Zhang[b], Jinbao Zhao[a,b,*]

[a] State Key Lab of Physical Chemistry of Solid Surfaces, College of Chemistry and Chemical Engineering, Collaborative Innovation Center of Chemistry for Energy Materials, State-Province Joint Engineering Laboratory of Power Source Technology for New Energy Vehicle, Xiamen University, Xiamen 361005, China
[b] College of Energy, Xiamen University, Xiamen 361102, China

ARTICLE INFO

Article history:
Received 27 February 2017
Received in revised form 29 March 2017
Accepted 29 March 2017
Available online 15 April 2017

Keywords:
L523
LMO
LFP
Electrolyte
Thermal stability

ABSTRACT

The thermal stabilities of delithiated $LiNi_{0.5}Co_{0.2}Mn_{0.3}O_2$ (L523), delithiated $LiMn_2O_4$ (LMO), and delithiated $LiFePO_4$ (LFP) for lithium ion batteries with bare electrode, solvent and different concentration of electrolyte under delithiated state have been investigated by using differential scanning calorimetry (DSC) and ex X-ray diffraction (XRD). The LFP has the best thermal stability, follows by the LMO and then the L523. The existing of solvent facilitates the decomposition of materials. The addition of Li salt in solvent can further accelerate the thermal decomposition of LMO and LFP; but hold back the decomposition of L523 at some extent that although the total reaction heat grown by 297 J g^{-1}, the first exothermic peak (ca. 279 °C) moves backwards comparing with L523 and solvent coexisting system (ca. 255.7 °C). As increasing the ratio of electrode material quality to electrolyte, the total exothermic quantity of L523 and LMO becomes large, meanwhile the unit mass exothermic quantity of the L523 varies with little dropping tendency, and that of the LMO decreases obviously. However, for the LFP, the total exothermic quantity decreases and the unit mass exothermic quantity decreases more obviously. Also, the XRD patterns of the three samples at ambient temperature and after 350 °C processing with existing of solvent or electrolyte suggest that the L532, LMO and LFP suffer evident structure changes since their pristine peaks become broader, weaker and splitting or disappearing at high temperature.

1. Introduction

Due to its excellent energy density and easy portability than all other rechargeable cells, lithium ion batteries are now extensively applied in the portable digital electronic products such as camera, laptops and so on [1–10]. As extending the lithium ion battery to large electric vehicle, hybrid electric vehicle, plug-in hybrid electric vehicle, communications engineering and national defense fields, the performance, especially safety performance, becomes the first concern problem for the application of lithium ion batteries [11–16]. The safety problems existing in the electronic products may bring disastrous consequences for electric instruments.

As a result of rapid input of specific energy, at an extreme condition, the battery will be induced to occur internal physical or chemical reactions and produce a large amount of heat, causing the battery temperature rise rapidly, which will accelerate the reactions out of control, resulting in the thermal runaway of the battery [17,18]. There are studies shown that when the temperature of the lithium ion battery reaches to 80 °C, it is likely to trigger a thermal runaway, eventually leading to burning and explosion of the battery [19]. The experimental and simulation work of Maleki et al. [20,21] have indicated that the reactions between the cathode material and the liquid organic electrolyte govern the exothermal reaction behavior and finally result in a thermal runaway. Because of the high potential of cathode materials and flammable organic electrolyte, the explosion and burning questions are easy produced when the heat producing speed is faster than the cooling speed.

Since the rapid response between cathode materials and electrolyte is the main reason for the thermal runaway, exploring the essences of thermal property for popular cathode materials is

* Corresponding author at: State Key Lab of Physical Chemistry of Solid Surfaces, College of Chemistry and Chemical Engineering, Collaborative Innovation Center of Chemistry for Energy Materials, State-Province Joint Engineering Laboratory of Power Source Technology for New Energy Vehicle, Xiamen University, Xiamen 361005, China.
E-mail address: jbzhao@xmu.edu.cn (J. Zhao).
[1] Y. Yu and J. Wang contributed equally to this work and share the first authorship.

http://dx.doi.org/10.1016/j.est.2017.03.016
2352-152X/

particularly important to ensure the safety of the whole battery. The thermal stability of usual cathode coexisting with electrolyte has been widely investigated by calorimeter instruments and spectrometers. Xiang [22] explored the thermal behavior of several cathode materials by differential scanning calorimetry (DSC) and *in-situ* fourier transform infrared spectroscopy (FTIR) spectra, and Park [23] studied the thermal reactions of olivine at a broad temperature (50–700 °C) by XRD and DSC characterizations. The DSC behaviors of L523 [24], LMO [25], and olivine [23] have also been investigated by people. However, the exothermic peaks related to which components of electrolyte and the exothermic peaks whether or not related to the content of electrolyte are still undefined and ambiguous. Therefore, it is quite necessary to analyze the every exothermic peak of cathode coexisting with electrolyte by varying the components of electrolyte and exclusive method, which has important influence on improving the safety of Li-ion batteries in practical use.

In this work, we explore the thermal behaviors of several wide-used cathode materials including L523, LMO, and LFP with different lithium salt amounts, different ratios of electrolyte contents by DSC and ex-XRD. The relations between the cathode and electrolyte components as well as between each exothermic peak and electrolyte component amount for thermal stability are comprehensively investigated.

2. Experimental

2.1. Materials preparation

The L523 was obtained from Ningbo Jinhe New Materials Co., Ltd; the LMO was acquired from Qingdao LNCM Co., Ltd; and the LFP was purchased from Shenzhen Dynanonic Co., Ltd.

Preparation for the delithiated samples using for DSC/thermal gravity analysis (TGA) measurements were as follows. First, the button cell was tested for one cycle and then charged to full delithiated state (4.3 V) at 0.5C. Second, electrode pole piece was obtained by disassembling the charged cell in an inert atmosphere. Third, the pole piece was cleaned several times with dimethyl carbonate (DMC) and spontaneously dried in an inert atmosphere. Finally, the material powders extracted from pole piece and electrolyte were encapsulated in company in a gold-plated stainless steel crucible in an inert atmosphere. The ratio of electrode materials to electrolyte was 1 mg of electrode materials per milliliter electrolyte. In the course of DSC test, the stainless steel crucible system was keeping in a sealed state without air contact and quality loss.

2.2. Materials characterization

Rigaku miniflex 600 were used to obtain the XRD results with Cu Kα radiation ran at 40 kV and 15 mA sweeping from 10° to 90° at 2° min^{-1} with 0.02° step size. The morphology of materials were portrayed by the field emission scanning electron microscopy (SEM, HITACHI S-4800), and the surface elemental distribution of particles were got by the energy dispersive X-ray spectroscopy (EDS, OXFORD 7593-H, an appendage of SEM) with an acceleration voltage of 20 kV. The thermal behaviors of electrode materials were gained by the DSC/thermogravimetry (TG) (STA 449 F3 Jupiter Netzsch) from 50 °C to 350 °C by 5 °C min^{-1} heating speed.

In DSC and ex-XRD tests, the blending solvent of ethylene carbonate (EC) and DMC with the weight ratio of 1: 1 is denoted as solvent, the electrolyte consisting of 1 M $LiPF_6$ salt dissolved in a mixture solvent of EC and DMC with the weight ratio of 1: 1 is marked as 1 M electrolyte, and the electrolyte consisting of 2 M $LiPF_6$ salt dissolved in a mixture solvent of EC and DMC with the weight ratio of 1:1 is labelled as 2 M electrolyte.

2.3. Electrochemical measurements

The electrochemical performances of all samples were assessed by using a CR2016 coin- type cells. The electrode plate was got by unfolding a sizing agent consisting of 85 wt% active material, 8 wt% acetylene black, 2 wt% graphite black and 5 wt% polyvinylidene difluoride (PVDF) binder scattered in 1-methyl pyrrolidione liquid

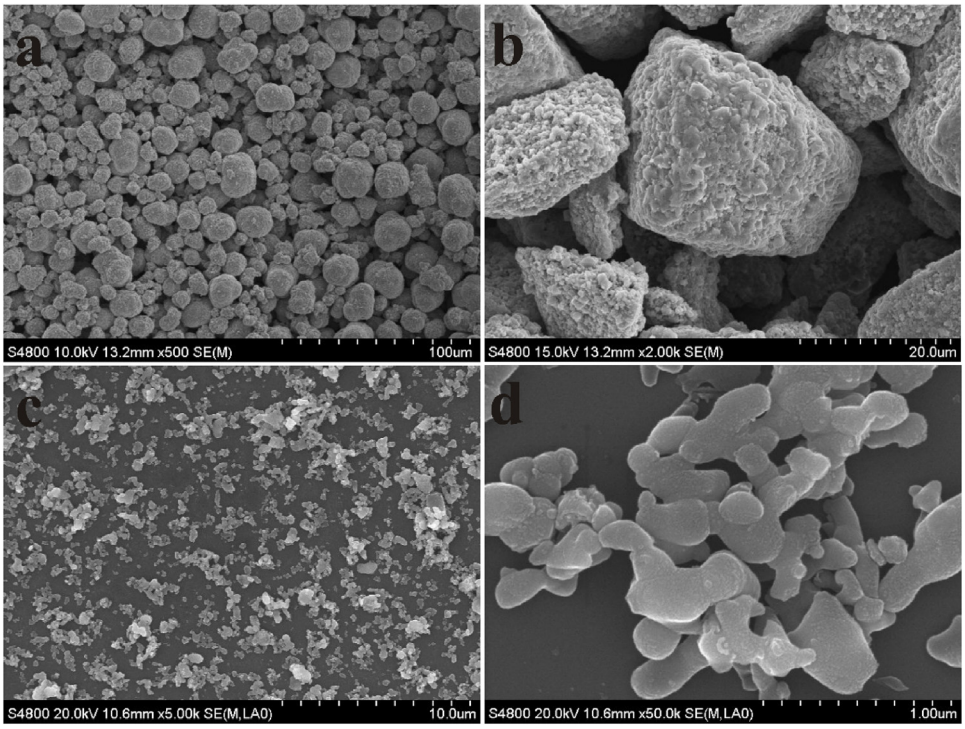

Fig. 1. SEM pictures of L523 (a), LMO (b) and LFP (c–d).

onto the surface of aluminum foil by using a coating machine. The 12 mm electrode was punched by a mold, pressed at 10 tons/1.13 cm^2 and dried in a vacuum oven at 100 °C for 12 h to remove residual solvent and water. The evaluated CR2016 button cells were fabricated by intercalating a porous polyethylene separator between the Li metal foil and electrode in an Ar-filled glove box. The electrolyte during electrochemical test was 1.0 M $LiPF_6$ salt dissolved in a mixture solvent of EC/DMC (w/w, 1:1).

A constant current and constant voltage charging pattern (CC-CV) and specific constant current discharging model were used for batteries between 3.0–4.3 V at ambient temperature on the NEWARE BTS type battery charger (Shenzhen, China). For instance, the batteries were first charged by constant current to 4.3 V at 1C, and after arriving 4.3 V the voltage was held at 4.3 V until the current reduced slowly to one-tenth of constant current process. The current values at all sorts of rates were configured on account of the practical capacity of the L523 (150 mAh g^{-1}), LMO (110 mAh g^{-1}) and LFP (150 mAh g^{-1}). All the tests were proceeded at room temperature unless otherwise stated.

3. Results and discussion

3.1. Structural representation and electrochemical behavior

The SEM graphs of the L523 (a), LMO (b), and LFP (c,d) samples are presented in Fig. 1, respectively. The L523 particles are sphere-like shapes in a size ranging from 4 μm to 10 μm (Fig. 1a). The LMO are irregular large particles (Fig. 1b), between 10 μm and 40 μm. The LFP (Fig. 1c–d) are flake-like submicron particles, ca. 200–500 nm.

The XRD figure of the commercial sample powders is portrayed in Fig. 2. The L523 display a specific layer structure belonging to a hexagonal $NaFeO_2$ structure (a $R\bar{3}m$ lattice spacing) without impure peaks appearing, [6] the LMO exhibit a spinel structure basing on Fd3 m space group, and the LFP present an orthogonal olivine structure pertaining to Pnma space group. There are no impurity peaks emerged in all three materials, indicating that the crystal forms of the three sample are excellent.

The first charging-discharging curves of the three materials at 0.5 C with the voltage ranging from 3.0 to 4.3 V are shown in Fig. 3. The L523 has experienced two processes in charge/discharge processes, corresponding to the redox of Ni^{2+}/Ni^{3+} (3.7–3.9 V) and Ni^{3+}/Ni^{4+} (3.9 V to 4.4 V). The plateaus of L523 is not obvious with a sequential voltage decreasing appearance which is the feature of layer structure for $LiNi_xCo_yMn_{1-x-y}O_2$ [6]. The first charging and discharging capacities of the L523 are 176.6 mAh g^{-1} and 151.7 mAh g^{-1}, respectively, with the coulomb efficiency of

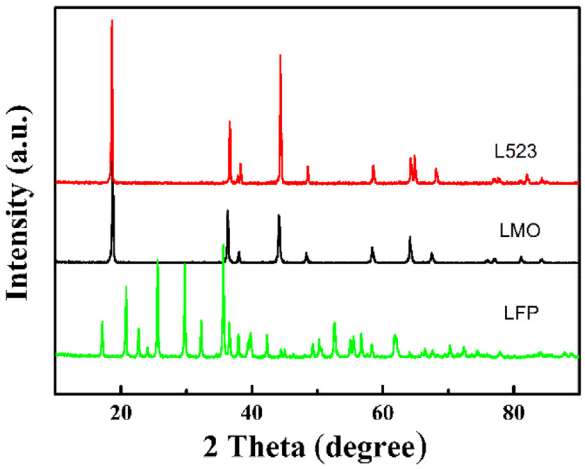

Fig. 2. XRD pattern of samples.

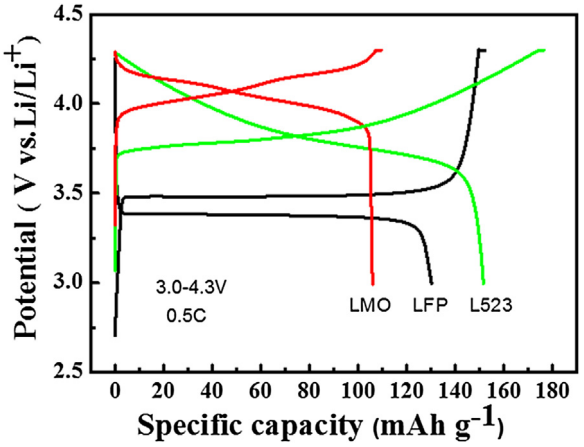

Fig. 3. First charge-discharge curves of materials at 0.5C at 3.0–4.3 V.

86.0%. The low coulomb efficiency of the L523 in first cycle is generally considered as the following two reasons. One view is the solid electrolyte interphase (SEI) formation on the surface of the electrode or inadequate infiltration between electrode materials and electrolyte [26]. Another view is that lithium ions beyond 3a position can not intercalate back into material after deintercalating from crystal lattice [27]. Two plateaus locating at 3.9 V and 4.1 V are observed for the LMO. The first charging and discharging capacities of the LMO are 109.5 mAh g^{-1} and 106.1 mAh g^{-1}, respectively, with the high coulomb efficiency up to 96.9%, which means good reversibility. There is an obvious platform near 3.5 V for the LFP, corresponding to the redox of Fe^{2+}/Fe^{3+}. The first charging and discharging capacities of the LFP are 152.2 mAh g^{-1} and 130.2 mAh g^{-1}, respectively, with the coulomb efficiency of 85.5%.

3.2. Thermal analysis

3.2.1. Electrolyte

The DSC curves of pure 1 M electrolyte and bare solvents free from Li salt are shown in Fig. 4. The electrolyte has an obvious exothermic peak, the initial exothermal temperature is 262.2 °C and the peak is at 281.2 °C, while for the solvent at 100–350 °C range there is no apparent heat release, indicating that the addition of $LiPF_6$ arouses some exothermic reactions between lithium salts and solvents.

In the heating process, the PF_5 (a strong Lewis acid) is produced by $LiPF_6$ decomposition and the PF_5 will offend the lone pair

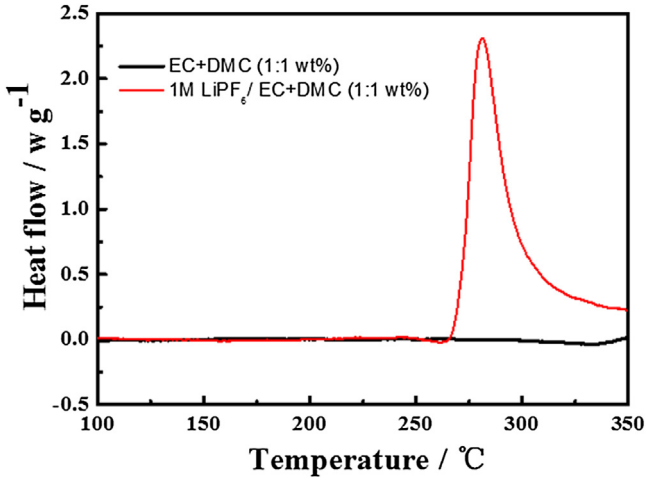

Fig. 4. DSC curves of 1 M electrolyte and solvents (EC + DMC) at 5 °C min^{-1} heating rate.

electrons of oxygen atoms in the EC, which will result in the destroying of loop structure and then the ring-opening reaction will happen, and finally, the above reaction products will occur polymerization, such as Eqs. (1)–(3) shown, accompanying heat release. Meanwhile, the PF_5 will react with trace water in electrolyte, resulting in corrosive HF. This series of reactions lead to the poor thermal stability of electrolyte [28–30].

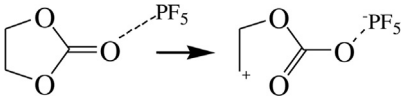

(1)

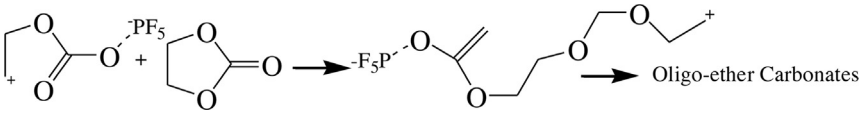

(2)

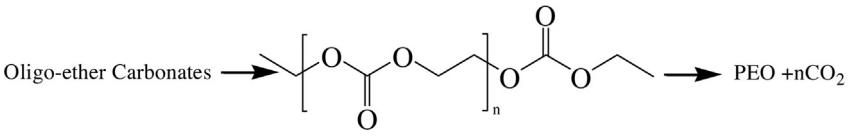

(3)

3.2.2. L523

The thermal stability of delithiated L523 (charged to 4.3 V) without electrolyte was studied by DSC/TG test as shown in Fig. 5a. Heat quantity of bare L523 is very small, the biggest heat flow is only 0.7 W g^{-1}, and exothermic peak locates at 331.4 °C. The DSC results of the delithiated L523 electrode coexisting with solvent, the 1 M electrolyte and the 2 M electrolyte, respectively, with the ratio of 1 mg: 1 μL are displayed in Fig. 5b. As adding solvent into delithiated L523 system, the thermal stability of system decreases obviously since the exothermic peak temperature declines from 331.4 °C to ca. 255.7 °C and the biggest heat flow rises from 0.7 W g^{-1} to 4.0 W g^{-1}. The heat release of L523 coexisting with the 1 M electrolyte is up to 1234 J g^{-1}. This is because delithiated L523 is unstable at high temperatures with O_2 releasing which will oxidize solvents and sent out a lot of heat. Meanwhile the reducing environment of solvent can promote the decomposition of L523, causing the exothermic peak emerged in advance. For the L523 and the 1 M electrolyte coexisting system, the first exothermic peak (ca. 279 °C) moves backwards comparing with L523 and solvent coexisting system (ca. 255.7 °C), which illustrate the addition of lithium salt into solvent has certain inhibitory effect on the oxidation reaction of delithiated L523 with solvent. This is because the L523 can lower the HF amount in electrolyte by Li^+/H^+ exchange at 160–200 °C, while the LMO can not reduce the HF content, so a series of reactions will happen, leading the exothermic peak in advance [11].

Two exothermic peaks appear in the L523 and the 1 M electrolyte coexisting system. When the Li salt concentration is increased to 2 M, the total Reaction heat increases by 173 J g^{-1}, the first peak area grows, and the second peak area decreases accompanying by maximal heat flow dropping from 9.8 to 5.2 W g^{-1}, which suggest the first peak is related to the amount of $LiPF_6$. The first peak consumes the L523 content, because the L523 amount is excess comparing with Li salt during reaction. Baba's study [31] also suggests there are two exothermic peaks for $Li_{0.49}CoO_2$ and electrolyte coexisting system in DSC curve, and the low peak is attributed to the oxidization of solvent on the surface of material. The second peak area decreases because the first peak makes some L523 reduction, resulting in reducing the amount of O_2 releasing in the back process. Meanwhile the solvent in the system is excess, and the heat quantity of oxidizing solvent is reduced. The specific data are shown in Table S1.

According to our previous study, the exchange reaction occurs between H^+ from HF and Li^+ in the L523 [11]. Therefore, if H^+ enters into the crystal lattice of the material, once encountering with the electrons produced by solvent oxidization on the surface of material, the material will be reduced and produce H_2O at the same time. When the temperature exceeds 200 °C, the H_2O releasing from body phase will react with PF_5 produced by $LiPF_6$ decomposition to generate more H^+, then the above reactions will continue. The increasing of $LiPF_6$ will result in the growth of generated H^+, so the first peak will grow along with the increasing of $LiPF_6$ content. Meanwhile, at this temperature the exothermic reaction also occurs by electrolyte itself, therefore, the first exothermic peak should be attributed to both the oxidation reaction between material and electrolyte and the reaction by electrolyte itself.

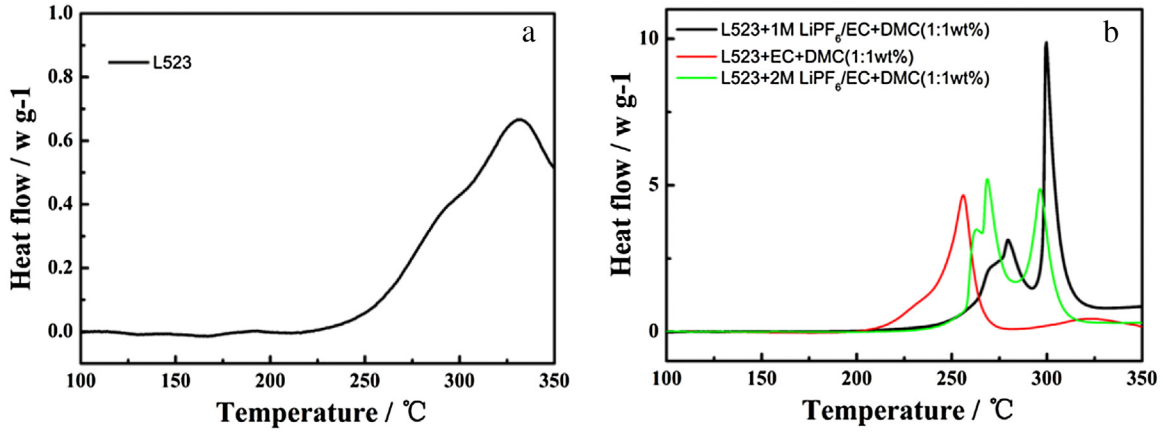

Fig. 5. DSC curves of (a) bare delithiated L523 (charged to 4.3 V), (b) delithiated L523 (charged to 4.3 V) coexisting with bare solvent, 1 M electrolyte and 2 M electrolyte in a sealed crucible.

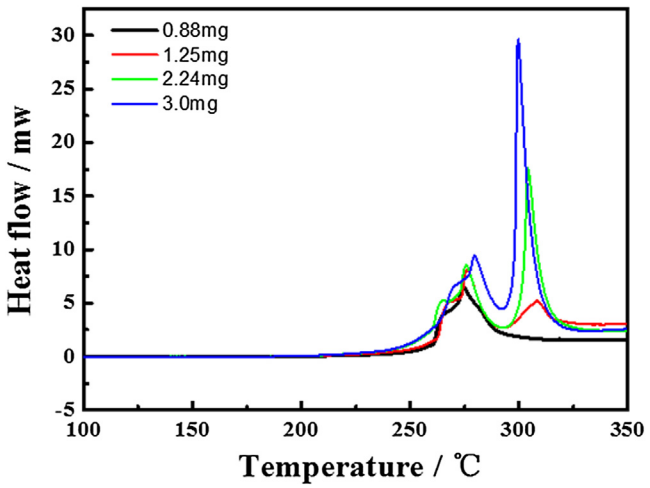

Fig. 6. DSC profiles of delithiated L523 in 3 μL electrolyte with different weights.

In order to further investigate the effect of Li salt and electrolyte amounts on the thermal stability of L523, we studied the thermostability of different L523 contents in 3 μL electrolyte shown in Fig. 6. With the increasing of L523 amount, the first exothermic peak has little changes and the second peak grows stronger, which further suggest the first peak is related to the $LiPF_6$ amount. The first peak undergoes little changes along with the increase of L523 since the $LiPF_6$ amount is the same in the 3 μL electrolyte closed system. Meanwhile the second peak area increases, because the increasing content of L523 will release more O_2 to oxidize solvents. The heat quantity of each system is presented in Table S2, showing that with the increasing of L523 content, the total heat quantity grows, and heat quantity of unit mass has a small decreasing tendency.

3.2.3. LMO

The DSC curve of bare delithiated LMO is shown in Fig. 7a. The heat quantity of bare LMO is very small, only 0.4 $W g^{-1}$, and exothermic peak is located at 269.9 °C. The thermal performance of delithiated LMO coexisting with solvent, the 1 M electrolyte and the 2 M electrolyte with the ratio of 1 mg: 1 μL are presented in Fig. 7b. [11] The detailed data are presented in Table S3. For the delithiated LMO/solvent system, an intense exothermic reaction occurs at 243.6 °C with the 4.968 $W g^{-1}$ heat flow, which is attributed to the reaction between solvent and O_2 released by LMO decomposition at high temperature.

After addition of $LiPF_6$ in solvent, the initial exothermal temperature of LMO/electrolyte system significantly decreases. When the concentration of $LiPF_6$ is increased from 1 M to 2 M, the onset exothermal temperature is dropped from 162.4 to 157.6 °C, and total quantity of heat grows from 1157 J g^{-1} to 1447 J g^{-1}. Also, the heat flow between 160 and 200 °C rises, while the exothermic peak area around 270 °C decreases. This is because that the exothermic behavior between 160 and 200 °C is connected to the HF amount in electrolyte, [11] and the increasing of Li salt concentration results in the growth of HF in electrolyte, so the heat flow before 200 °C rises along with Li salt concentration increasing. The exothermic behavior between 160 and 200 °C expends some LMO, which leads to the reducing of the releasing O_2 content, so the heat quantity around 270 °C decreases. In general, although LMO/electrolyte has lower onset exothermic temperature than L523/electrolyte, the heat quantity release of LMO/electrolyte system is far less than that of L523, especially for the heat flow, therefore, the thermal stability of LMO is better than L523.

The DSC profiles of 3 μL electrolyte with different quality of delithiated LMO (charged to 4.3 V) are shown in Fig. 8. With the increasing of electrode material quality, the behavior of LMO is obvious different from that of the L523. The onset exothermic temperature moves to low temperature, which may be ascribed to the combined action of HF in electrolyte and decomposition product of electrolyte. Generally, there are three peaks of the LMO/electrolyte coexisting system for DSC curves. However, when the quantity of LMO is small, the peak around 270 °C disappears, which

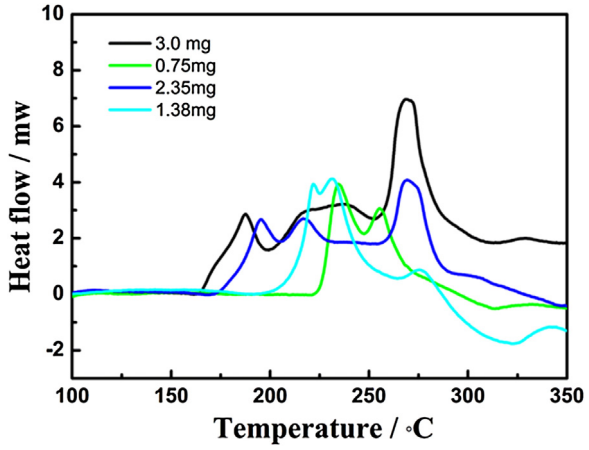

Fig. 8. DSC profiles of delithiated LMO in 3 μL electrolyte with different weight.

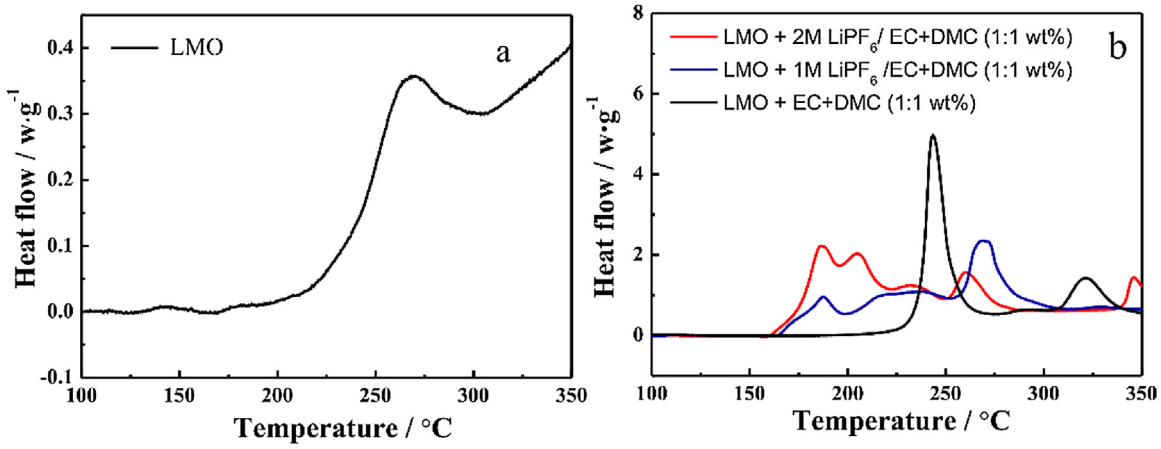

Fig. 7. DSC curves of (a) delithiated LMO; (b) delithiated LMO coexisting with solvent, 1 M electrolyte and 2 M electrolyte.

may be attributed that these little LMO is all consumed before 270 °C by the reaction between material and electrolyte. Therefore, for 0.75 mg LMO coexisting with 3 μL electrolyte system, there are only two exothermal peaks appearing. With the LMO amount increasing, the peak area at 270 °C increases gradually, which is related to the further oxidation reaction between the LMO and electrolyte. The detailed thermal data of the 3 μL electrolyte with different quality of the LMO are shown in Table S4. It is can be seen that along with increase of the LMO quality in the closed system, the total heat quantity increases, but the heat release of unit mass electrode material reduces.

3.2.4. LFP

The thermal behavior of delithiated LFP (charged to 4.3 V) is exhibited in Fig. 9a, which suggests a good thermal stability of bare LFP without any apparent heat peak appearing among 100–350 °C. The DSC curves of delithiated LFP together with solvent, the 1 M electrolyte and the 2 M electrolyte with the ratio of 1 mg: 1 μL are presented in Fig. 9b. The LFP/solvent coexistence system has good thermal stability, and the initial exothermic temperature is above 330 °C which may be ascribed to the oxidation of electrolyte.

For the LFP coexisting with the 1 M electrolyte system, the initial exothermal temperature is decreased to 225 °C, which illustrates the joining of lithium salt is disadvantageous to the thermal stability of the system. With the lithium salt concentration increasing from 1 M to 2 M, the peak between 225 and 325 °C grows, and the total heat quantity increases from 525 J g^{-1} to 781 J g^{-1}, which may be associated with lithium salt content. Comparing the thermal behaviors of LFP/1 M electrolyte system with the bare solvent system (Fig. 4), it can be seen that the joining of LFP can slow the catalytic decomposition of electrolyte itself, so the heat flow becomes relatively small, also the heat quantity is less than the single electrolyte, although the addition of LFP make the initial exothermal temperature in advance.

The DSC results of 3 μL electrolyte accompanying with different qualities of LFP (charged to 4.3 V) are shown in Fig. 10. The specific thermodynamic data of 3 μL electrolyte/LFP system are shown in Table S5. With the increasing of LFP amount, the initial exothermal temperature has no obvious change, but total heat has a tendency to decrease, and the heat release of unit mass electrode materials reduces more obviously. This is different with that of the LMO and the L523. Similar results are also reported by Xiang, [22] that LFP can suppress the decomposition of electrolyte because of the presence of covalent bonds [23] existing in its structure. People believe that the Lewis acid PF_5 in the electrolyte is captured by some reactive groups (e.g. unsaturated PO_4^{3-}) on the surface of LFP, which can catalyze electrolyte decomposition [32].

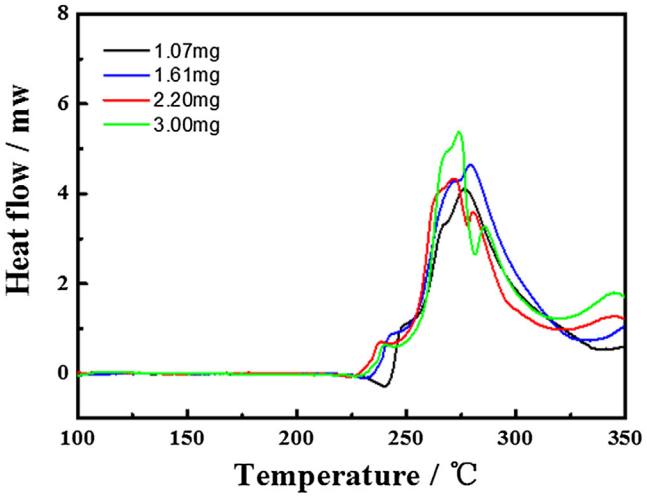

Fig. 10. DSC curves of delithiated LFP in 3 μL electrolyte with different weights.

3.3. Ex-XRD technology research for the structure changes of materials at high temperature

In order to further study the structural changes of fully delithiated material with solvent and different concentration of

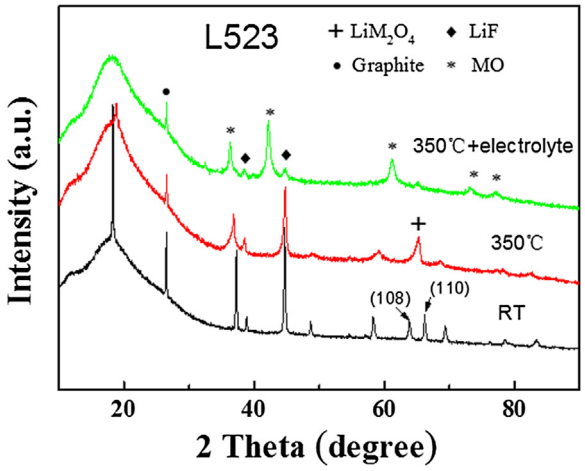

Fig. 11. Ex-XRD data of delithiated L523 at ambient temperature and L523 coexisting with or without electrolyte at 350 °C.

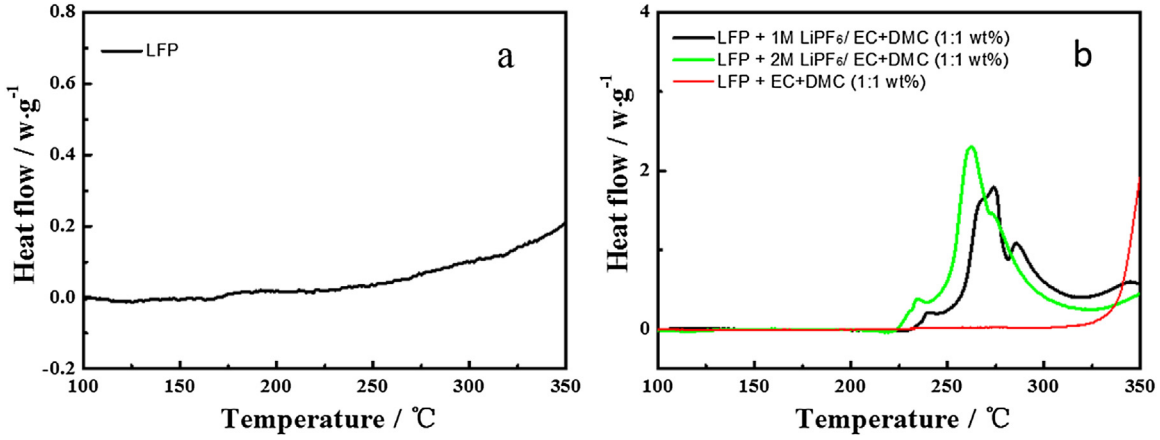

Fig. 9. DSC curves of (a) LFP (charged to 4.3 V); (b) delithiated LFP coexisting with solvent, 1 M electrolyte and 2 M electrolyte.

electrolyte at high temperature, the delithiated materials coexisting with the bare organic solvents or the electrolyte were first heated to 350 °C at a sealed state with the DSC test method and then spontaneously cooled to ambient temperature. Finally, the related reactive products are got out from the closed crucible in an inert atmosphere and covered with polyimide tape on carry sheet glass to hold back direct touching water and air during measuring process. The ex-XRD curve of delithiated L523 at ambient temperature labeling as RT, the delithiated L523 at 350 °C marking as 350 °C, and the delithiated L523 together with electrolyte system at 350 °C denoting as 350 °C + electrolyte are presented in Fig. 11. It is can be seen that for 350 °C sample (in the absence of electrolyte at 350 °C), the original separate (108) and (110) peaks merge into a peak, which illustrates the formation of spinel LiM_2O_4 phase. For the L523 coexisting with electrolyte, its structure has obvious changes. There are a lot of new phases formed, such as MO and LiF, which suggest that the electrolyte promotes the decomposition of material, the L523 is decomposed into MO rock salt phase, and the LiF is generated by $LiPF_6$ decomposition. All these results are consistent with Cho's [24] reports.

The preservation of delithiated LMO structure coexisting with or without electrolyte at high temperature were proved by ex-XRD shown in Fig. 12. In the absence of electrolyte, the bare material is partly decomposed into Mn_3O_4, which is in accordance with Yang's results [33]. The formation of Mn_3O_4 implies that the average valence state of Mn state decreases, illustrating the reduction of Mn. It may be attribute that redox reaction happens between conducting agent (C, acetylene black) in the electrode material or binder (PVDF) and delithiated LMO. Yang's mass spectrometry results have shown the generation of CO_2 generated at this temperature. In the presence of electrolyte, the delithiated LMO is further decomposed into MnO (JCPDS No.01-075-0625), Mn_2O_3 (JCPDS No.006-0540) and $MnCO_3$ (JCPDS No.01-086-0172) *etc*. This is because the presence of solvent can provide a rich electronic environment, which bring out that the delithiated LMO is easy access to electrons, accompanying the oxidation of electrolyte. The generation of MnF_2 (JCPDS No. 01-080-2217) is caused by $LiPF_6$ decomposition. The PF_5 decomposition product of $LiPF_6$ reacts with trace of water in electrolyte to produce the HF, and HF will react with MnO generated by delithiated LMO decomposition to form MnF_2.

The ex-XRD results of delithiated LFP coexisting with or without electrolyte at 350 °C are shown in Fig. 13. The results show that the structure of single LFP material does not happen obvious change after heated to 350 °C, so the bare LFP shows good thermal stability.

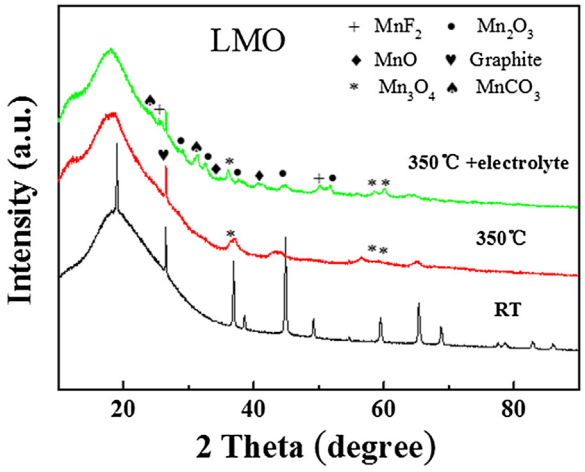

Fig. 12. Ex-XRD data of bare delithiated LMO at ambient temperature and delithiated LMO coexisting with or without electrolyte at 350 °C.

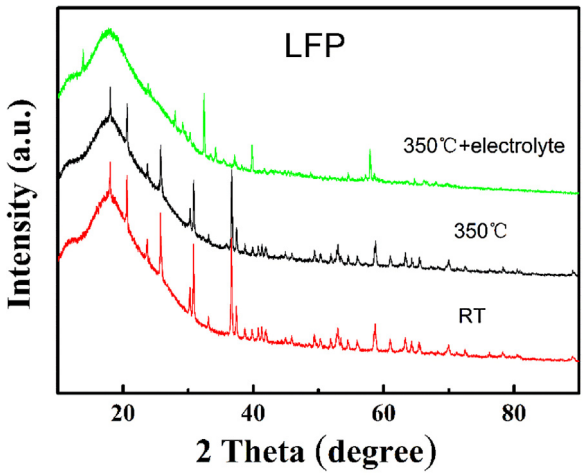

Fig. 13. Ex-XRD data of delithiated LFP at ambient temperature and delithiated LFP coexisting with or without electrolyte at 350 °C.

However, the LFP coexisting with electrolyte system after heated to 350 °C, the great changes have taken place. The research results suggest that the LFP may decompose into $Fe_2P_2O_7$ [23] at 350 °C due to the catalytic effect of the electrolyte. Comparing Figs. 9 and 13, it is can be concluded that although accompanying phase transformation during heat process, the delithiated olivines behave good thermally stable because of the presence of covalent bonds [23] existing in its structure.

4. Conclusions

In this work, we presented a systemic study for the thermal stability of delithiated L523, delithiated LMO and delithiated LFP with solvent and electrolyte of varying concentration. It has been preliminarily revealed by varying the components of electrolyte and exclusive method that the exothermic peaks whether or not related to the amount of electrolyte and which components of electrolyte were responsible for the exothermic peaks. The LFP has the best thermal stability, followed by the LMO and the L523 of the worst. The existence of solvent promoted the decomposition of materials. The addition of Li salt in solvent could further accelerate the thermal decomposition of LMO and LFP; but impeded the decomposition of L523 at some extent that although the total reaction heat increases by 297 J g^{-1}, the first exothermic peak (ca. 279 °C) shifted backwards comparing with L523 and solvent coexisting system (ca. 255.7 °C). As increasing the ratio of electrode material quality to electrolyte, the total exothermic quantity of L523 and LMO turned large, meanwhile the unit mass exothermic quantity of the L523 changed with little declining tendency, and that of the LMO dropped obviously. However, for the LFP, the total exothermic quantity decreased and the unit mass exothermic quantity decreased more obviously. Also, the XRD patterns of the three samples at ambient temperature and to be heated to 350 °C with existing of solvent or electrolyte indicated that the L532, LMO and LFP suffered evident structure changes since their pristine peaks became broader, weaker and splitting or disappearing after heated to 350 °C.

(1) For the bare materials: after heated to 350 °C, the LFP has the best thermal stability, followed by the LMO and then the L523. After heated to 350 °C, the structure of LFP did not happen any change and the LMO mainly kept basic structure with a small amount of Mn_3O_4 generating, which might be the result of redox reactions between LMO and carbon in cathode, but for the L523, it transformed to spinel phase.

(2) Comparing with the bare materials, the material and solvent coexisting system has larger heat flow and larger total heat release, suggesting the addition of solvent promotes the decomposition of materials.
(3) In the material and electrolyte coexisting system, the addition of Li salt could further promote the decomposition of LMO and LFP, but inhibited the decomposition of L523 to some extent. Although the total reaction heat increased by 297 J g^{-1}, the first exothermic peak (ca. 279 °C) of L523 and the 1 M electrolyte coexisting system moved backwards comparing with that of the L523 and solvent coexisting system which may be attributed that the L523 can lower the HF amount in electrolyte by Li^+/H^+ exchange. The first peak area was related to the $LiPF_6$ amount, while the second peak area was bound up with L523 amount positively. For the LMO, the heat flow before 200 °C rose along with Li salt concentration increasing and the heat quantity around 270 °C shown a positive correlation to the LMO amounts. For the LFP, the peak between 225–325 °C was positively associated with lithium salt content. The addition of LFP can slow the catalytic decomposition of electrolyte itself because of the presence of covalent bonds existing in its structure, so the heat quantity was even less than that of the single electrolyte, although the addition of LFP made the initial exothermal temperature in advance.
(4) Adding different quality of electrode materials in 3 μL electrolyte, the DSC results shown that with the raising of electrode material quality, the total exothermic quantity of L523 and the LMO turned large; but the exothermic quantity of the unit mass for the L523 changed little, and that for the LMO decreased obviously. The total exothermic quantity of the LFP decreased, and the exothermic quantity of unit mass decreased more obviously. Therefore, on the premise of guarantee the battery performance, less electrolyte should be used in lithium ion batteries as far as possible.
(5) In the electrolyte and electrode system at high temperature, the L523 decomposed into rock salt phase MO, the delithiated LMO decomposed into MnO, Mn_2O_3 and $MnCO_3$; and the LFP may decompose into $Fe_2P_2O_7$ due to the catalytic effect of the electrolyte.

Acknowledgments

This work was financial supported by National Natural Science Foundations of China (21603179, 21321062), and the Fundamental Research Funds for the Central Universities (No. 20720170021, No. 20720160082). The authors also wish to express their gratitudes to Prof. Daiwei Liao for his writing suggestions.

Appendix A. Supplementary data

Supplementary data associated with this article can be found, in the online version, at http://dx.doi.org/10.1016/j.est.2017.03.016.

References

[1] J. Yuan, J. Wen, J. Zhang, D. Chen, D. Zhang, Influence of calcination atmosphere on structure and electrochemical behavior of $LiNi_{0.6}Co_{0.2}Mn_{0.2}O_2$ cathode material for lithium-ion batteries, Electrochim. Acta 230 (2017) 116–122.
[2] Y. Yang, D. Chen, B. Liu, J. Zhao, Binder-free Si nanoparticle electrode with 3D porous structure prepared by electrophoretic deposition for lithium-Ion batteries, ACS Appl. Mater. Interfaces 7 (2015) 7497–7504.
[3] J. Wang, W. Lin, B. Wu, J. Zhao, Porous $LiNi_{0.5}Mn_{1.5}O_4$ sphere as 5 V cathode material for lithium ion batteries, J. Mater. Chem. A 2 (2014) 16434–16442.
[4] J. Wang, W. Lin, B. Wu, J. Zhao, Syntheses and electrochemical properties of the Na-doped $LiNi_{0.5}Mn_{1.5}O_4$ cathode materials for lithium-ion batteries, Electrochim. Acta 145 (2014) 245–253.
[5] J. Wang, S. Yao, Y. Yu, T. Fu, P. Zhang, J. Zhao, Improving the stability properties of 5 V lithium nickel manganese oxide spinel by surface coating with cobalt aluminum oxides for lithium ion batteries, Electrochim. Acta 208 (2016) 310–317.
[6] J. Wang, Y. Yu, B. Li, T. Fu, D. Xie, J. Cai, J. Zhao, Improving the electrochemical properties of $LiNi_{0.5}Co_{0.2}Mn_{0.3}O_2$ at 4.6 V cutoff potential by surface coating with Li_2TiO_3 for lithium-ion batteries, Phys. Chem. Chem. Phys. 17 (2015) 32033–32043.
[7] J. Wang, Y. Yu, B. Wu, W. Lin, J. Li, J. Zhao, A homogeneous intergrown material of $LiMn_2O_4$ and $LiNi_{0.5}Mn_{1.5}O_4$ as a cathode material for lithium-ion batteries, J. Mater Chem. A 3 (2015) 2353–2360.
[8] B. Li, Y. Yu, J. Zhao, Facile synthesis of spherical $xLi_2MnO_3\cdot(1\text{-}x)Li(Mn_{0.33}Co_{0.33}Ni_{0.33})O_2$ as cathode materials for lithium-ion batteries with improved electrochemical performance, J. Power Sources 275 (2015) 64–72.
[9] B. Li, J. Wang, Z. Cao, P. Zhang, J. Zhao, The role of SnO_2 surface coating in the electrochemical performance of $Li_{1.2}Mn_{0.54}Co_{0.13}Ni_{0.13}O_2$ cathode materials, J. Power Sources 325 (2016) 84–90.
[10] Q. Wu, Y. Yin, S. Sun, X. Zhang, N. Wan, Y. Bai, Novel AlF_3 surface modified spinel $LiMn_{1.5}Ni_{0.5}O_4$ for lithium-ion batteries: performance characterization and mechanism exploration, Electrochim. Acta 158 (2015) 73–80.
[11] J. Wang, Y. Yu, B. Li, P. Zhang, J. Huang, F. Wang, S. Zhao, C. Gan, J. Zhao, Thermal synergy effect between $LiNi_{0.5}Co_{0.2}Mn_{0.3}O_2$ and $LiMn_2O_4$ enhances the safety of blended cathode for lithium ion batteries, ACS Appl. Mater. Interfaces 8 (2016) 20147–20156.
[12] P. Röder, B. Stiaszny, J.C. Ziegler, N. Baba, P. Lagaly, H.-D. Wiemhöfer, The impact of calendar aging on the thermal stability of a $LiMn_2O_4$–$Li(Ni_{1/3}Mn_{1/3}Co_{1/3})O_2$/graphite lithium-ion cell, J. Power Sources 268 (2014) 315–325.
[13] P. Röder, N. Baba, H.D. Wiemhöfer, A detailed thermal study of a Li $[Ni_{0.33}Co_{0.33}Mn_{0.33}]O_2$/$LiMn_2O_4$-based lithium ion cell by accelerating rate and differential scanning calorimetry, J. Power Sources 248 (2014) 978–987.
[14] J. Yi, C. Wang, Y. Xia, Comparison of thermal stability between micro and nano-sized materials for Lithium-ion batteries, Electrochem. Commun. 33 (2013) 115–118.
[15] Q. Wang, P. Ping, X. Zhao, G. Chu, J. Sun, C. Chen, Thermal runaway caused fire and explosion of lithium ion battery, J. Power Sources 208 (2012) 210–224.
[16] A.J. Smith, S.R. Smith, T. Byrne, J.C. Burns, J.R. Dahn, Synergies in blended $LiMn_2O_4$ and $Li[Ni_{1/3}Mn_{1/3}Co_{1/3}]O_2$ positive electrodes, J. Electrochem. Soc. 159 (2012) A1696–A1701.
[17] R.M. Spotnitz, J. Weaver, G. Yeduvaka, D. Doughty, E. Roth, Simulation of abuse tolerance of lithium-ion battery packs, J. Power Sources 163 (2007) 1080–1086.
[18] B.K. Mandal, A.K. Padhi, Z. Shi, S. Chakraborty, R. Filler, Thermal runaway inhibitors for lithium battery electrolytes, J. Power Sources 161 (2006) 1341–1345.
[19] A. Hammami, N. Raymond, M. Armand, Lithium-ion batteries: runaway risk of forming toxic compounds, Nature 424 (2003) 635–636.
[20] H. Maleki, J.N. Howard, Role of the cathode and anode in heat generation of Li-ion cells as a function of state of charge, J. Power Sources 137 (2004) 117–127.
[21] H. Maleki, G. Deng, I. Kerzhner-Haller, A. Anani, J.N. Howard, Thermal stability studies of binder materials in anodes for lithium-ion batteries, J. Electrochem. Soc. 147 (2000) 4470–4475.
[22] H.F. Xiang, H. Wang, C.H. Chen, X.W. Ge, S. Guo, J.H. Sun, W.Q. Hu, Thermal stability of LiPF6-based electrolyte and effect of contact with various delithiated cathodes of Li-ion batteries, J. Power Sources 191 (2009) 575–581.
[23] J.-S. Park, S.-M. Oh, Y.-K. Sun, S.-T. Myung, Thermal properties of fully delithiated olivines, J. Power Sources 256 (2014) 479–484.
[24] Y.-H. Cho, D. Jang, J. Yoon, H. Kim, T.K. Ahn, K.-W. Nam, Y.-E. Sung, W.-S. Kim, Y.-S. Lee, X.-Q. Yang, W.-S. Yoon, Thermal stability of charged $LiNi_{0.5}Co_{0.2}Mn_{0.3}O_2$ cathode for Li-ion batteries investigated by synchrotron based in situ X-ray diffraction, J. Alloys Compd. 562 (2013) 219–223.
[25] Q. Wang, J. Sun, C. Chen, Thermal stability of delithiated $LiMn_2O_4$ with electrolyte for lithium-ion batteries, J. Electrochem. Soc. 154 (2007) A263–A267.
[26] Z. Wang, Y. Sun, L. Chen, X. Huang, Electrochemical characterization of positive electrode material $LiNi_{1/3}Co_{1/3}Mn_{1/3}O_2$ and compatibility with electrolyte for lithium-ion batteries, J. Electrochem. Soc. 151 (2004) A914–A921.
[27] A. Rougier, I. Saadoune, P. Gravereau, P. Willmann, C. Delmasa, Effect of cobalt substitution on cationic distribution in $LiNi_{1-y}Co_yO_2$ electrode materials, Solid State Ion. 90 (1996) 83–90.
[28] Q. Wang, J. Sun, X. Yao, C. Chen, Thermal stability of $LiPF_6$/EC + DEC electrolyte with charged electrodes for lithium ion batteries, Thermochim. Acta 437 (2005) 12–16.
[29] M. Moshkovich, M. Cojocaru, H. Gottlieb, D. Aurbach, The study of the anodic stability of alkyl carbonate solutions by in situ FTIR spectroscopy, EQCM NMR and MS, J. Electroanal. Chem. 497 (2001) 84–96.
[30] S.E. Sloop, J.B. Kerr, K. Kinoshita, The role of Li-ion battery electrolyte reactivity in performance decline and self-discharge, J. Power Sources 119 (2003) 330–337.
[31] Y. Baba, S. Okada, J. Yamaki, Thermal stability of Li_xCoO_2 cathode for lithium ion battery, Solid State Ion. 148 (2002) 311–316.
[32] S.E. Sloop, J.B. Kerr, K. Kinoshita, The role of Li-ion battery electrolyte reactivity in performance decline and self-discharge, J. Power Sources 119–121 (2003) 330–337.
[33] E. Hu, S.M. Bak, S.D. Senanayake, X.-Q. Yang, K.-W. Nam, L. Zhang, M. Shao, Thermal stability in the blended lithium manganese oxide–lithium nickel cobalt manganese oxide cathode materials: an in situ time-resolved X-ray diffraction and mass spectroscopy study, J. Power Sources 277 (2015) 193–197.